Supporting Information

$Te/ZnIn_2S_4$ Nanoleaves with Rich Charge Transport and High Electron-hole Separation Efficiency for Augmented Visible-Light-Mediated Hydrogen Peroxide Generation

Fangzheng Qi,[a] Zengsheng Guo,*[,a] Cuiping Lin,[a] Chenchen Wang,[a] Guihua Jiang,[c] Yiqiang Sun,*[,a] Cuncheng Li,*[,a, b] and Lifeng Hang*[,c]

[a.] School of Chemistry and Chemical Engineering, University of Jinan, Jinan 250022, P. R. China.

[b.] Collaborative Innovation Center of Yellow River Basin Pharmaceutical Green Manufacturing and Engineering Equipment, University of Jinan, Jinan 250022, P. R. China.

[c.] Xiamen Humanity Hospital, Fujian Medical University No.3777 Xianyue Road, Xiamen City, Fujian Province, China

EXPERIMENTAL SECTION

Synthesis of Te NWs

Te nanowires were synthesized via a modified hydrothermal reduction process. Briefly, 0.1 g sodium tellurite (Na_2TeO_3) and 0.2 g polyvinyl pyrrolidone (PVP) were dissolved in 100 mL deionized water. Subsequently, 1.0 mL of hydrazine hydrate ($N_2H_4 \cdot H_2O$) and 2.0 mL of ammonia water (25-28 wt% of NH_3,) were dropped into the solution under vigorous stirring in the dark. The above solution was transferred and sealed into a Teflon-lined autoclave. The autoclave was heated to 180 ℃ for 3 h. Then the autoclave was cooled down naturally to room temperature. The product was centrifugated and washed sequentially by 50 mL of ethanol and water to remove any possible contaminations, and finally dried at 50 ℃ in a vacuum oven

Synthesis of $ZnIn_2S_4$ NPs

In a typical synthesis, 20 mL of H_2O and 3 mL of glycerol were injected into a 50 mL glass bottle. Then, the solution was sonicated for 10 min to obtain a uniform solution. Subsequently, 0.2 mmol $ZnCl_2$, 0.2 mmol $InCl_3 \cdot 4H_2O$ and 0.4 mmol thioacetamide were added to the above-mentioned solution and stirred for 30 min. The resulting mixture was allowed to heat at 80 ℃ for 2 h. After naturally cooling down to room temperature, the product was collected by centrifuging, washed with water and ethanol thoroughly, and dried at 40 ℃ in a vacuum.

Synthesis of Te/$ZnIn_2S_4$ NLs

In brief, 20 mg Te nanowires were ultrasonically dispersed in a mixed solution of 20 mL water and 3 mL glycerol. Subsequently, different amount of $InCl_3 \cdot 4H_2O$ (0.1, 0.2, 0.3 mmol), $ZnCl_2$ (0.1, 0.2, 0.3 mmol), and thioacetamide (TAA) (0.2 0.4, 0.6 mmol) were added to the solution and stirred for another 30 min to obtain a series of samples with different amount of $ZnIn_2S_4$. The resulting mixture was allowed to heat at 80 ℃ for 2 h. After naturally cooling down to room temperature, the product was collected by centrifuging, washed with water and ethanol thoroughly, and dried at 40 ℃ in a vacuum.The samples were then labeled as Te/ZIS-1, Te/ZIS-2, Te/ZIS-3 respectively.

Characterizations

The morphology and nanostructure were examined using transmission electron microscopy (TEM, JEM-1400) and high-resolution transmission electron microscopy (HRTEM, JEM-2100F). The composition of the product was analyzed by the accompanying energy dispersive spectroscopy (EDS). Concurrently, elemental profiling was conducted using the same instrumentation. The Philips X'pert Pro X-ray diffractometer was employed to obtain X-ray diffraction (XRD) spectra, while an ESCALAB 250 photoelectron spectrometer was utilized for X-ray photoelectron spectroscopy (XPS) analysis. In-situ diffuse reflection infrared Fourier transform spectroscopy (DRIFTS) analysis was performed in situ using a Nicolet iS50 FTIR spectrometer (Thermo Fisher, USA) to investigate the samples. Electron paramagnetic resonance (EPR) spectroscopy data were acquired using the Bruker A300 spectrometer. The photoelectrochemical performance of the specimens was assessed using a CHI 650E potentiostat (Shanghai Chenhua) configured with a three-electrode system.

Photocatalytic Production of H_2O_2

The prepared samples were tested to evaluate the performance of the photocatalytic H_2O_2 production. In the experimental setup, 20 mg of the photocatalyst was dispersed in 100 mL of deionized water. Prior to exposure to a Xe-lamp ($\lambda \geq 420$ nm), the solution underwent prestirring for a duration of 30 min and continuous oxygen flow (30 mL min^{-1}) into the Pyrex reactor. The quantification of H_2O_2 was conducted using UV-vis spectrophotometry with potassium titanium oxalate methods.

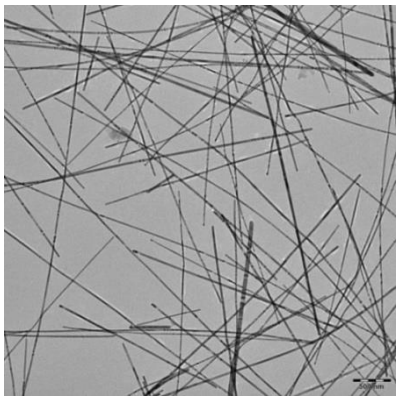

Fig. S1 TEM image of Te NWs.

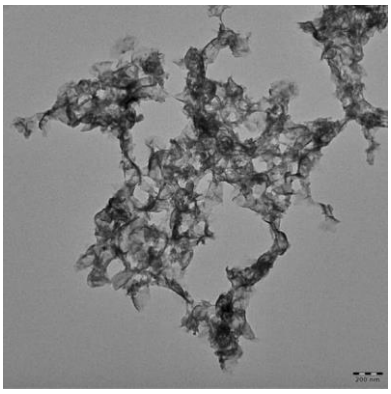

Fig. S2 TEM image of $ZnIn_2S_4$ NPs.

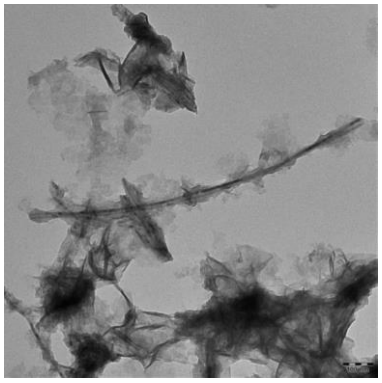

Fig. S3 TEM image of Te/ZIS NLs.

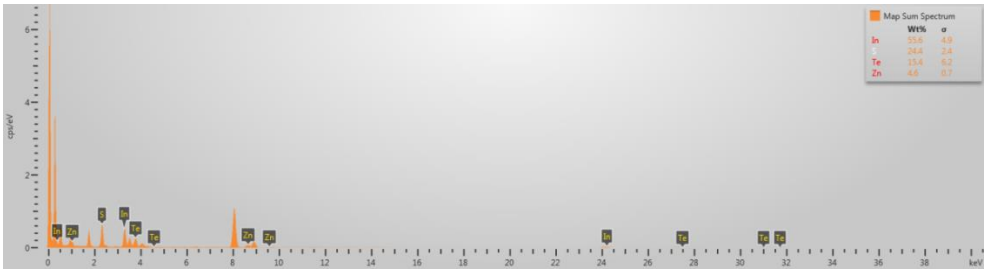

Fig. S4 EDS microanalysis spectrum of Te/ZIS NLs.

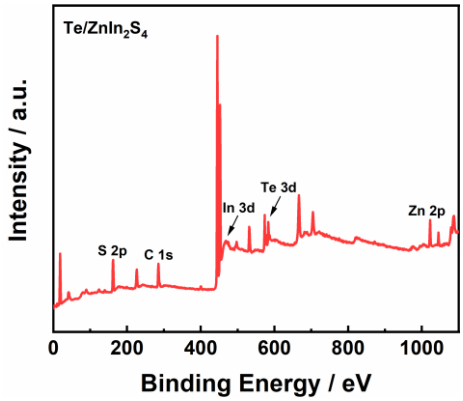

Fig. S5 XPS spectra of Te/ZIS NLs.

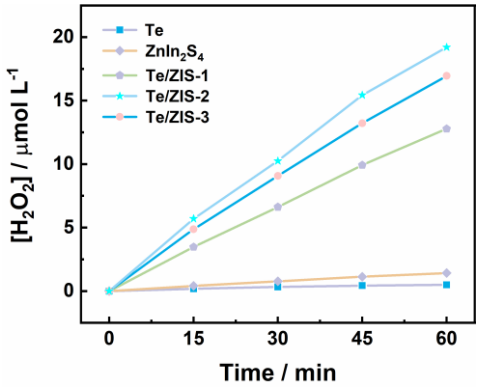

Fig. S6 Comparison of H_2O_2 yield.

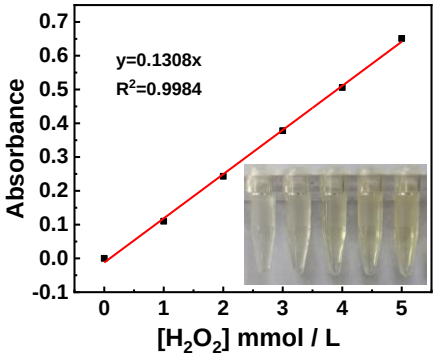

Fig. S7 Working curve for the determination of hydrogen peroxide concentration.

Using 0.5 mL of a quantifiable quantity of hydrogen peroxide solution, 1 mL of deionized water, and 1 mL of potassium titanium oxalate solution (0.05 mol L^{-1}), a calibration curve was created. When the concentration of hydrogen peroxide is above 10 mmol L^{-1}, the solution should be diluted to below 10 mmol L^{-1} before detection. The absorbance of the hydrogen peroxide color solution is then measured at 400 nm using UV-Vis.

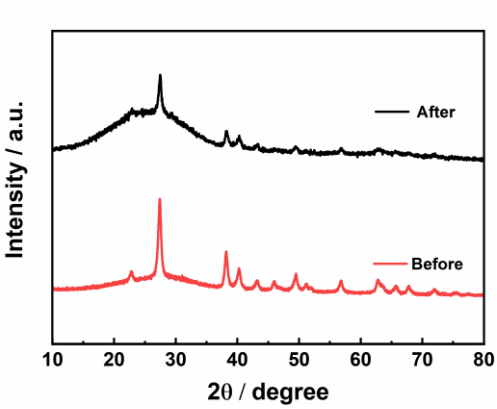

Fig. S8 XRD pattern of Te/ZIS NLs before and after used.

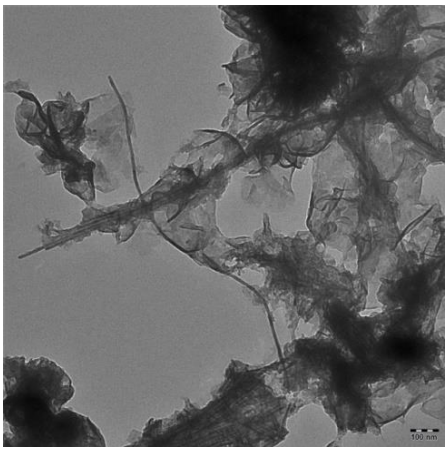

Fig. S9 TEM image of the recycled Te/ZIS NLs.

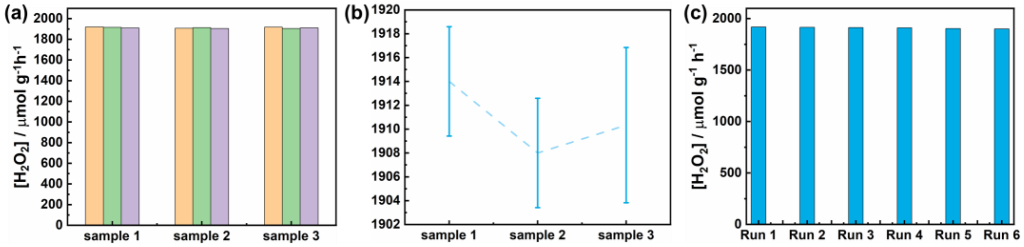

Fig. S10 (a) H_2O_2 production rate of the samples from five different batches, (b) Error analysis, (c) Stability test.

To validate reproducibility, we tested samples from three different batches, and the results exhibited minimal variation, further demonstrating the stability and repeatability of our synthesis and measurement processes. We also performed six-cycle stability tests. After six cycles, the H_2O_2 production rate showed a slight decline, which may be attributed to catalyst loss during the recovery process and a slight decrease in catalytic activity.

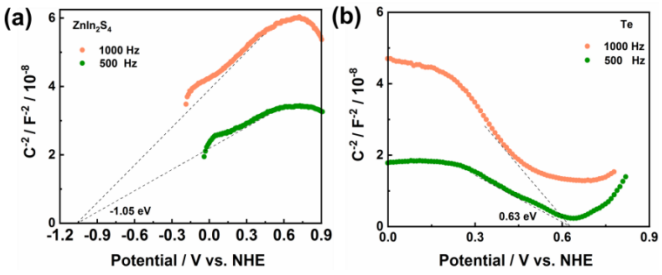

Fig. S11 M-S plots of (a) ZIS and (b) Te.

To probe the charge transfer dynamics between Te NWs and ZIS NPs, we conducted an in-depth analysis of the band structure using UV-vis diffuse reflection spectroscopy and Mott-Schottky analysis. The band gap (E_g) of ZIS and Te are 2.27 and 2.19 eV, respectively. The Mott-Schottky plots of ZIS and Te were shown in Fig. S11. For n-type semiconductor, the CB position usually more negative 0.1-0.3 eV than the flat band potential, while for p-type semiconductor, the VB position usually more positive 0.1-0.3 eV than the flat band potential. Therefore, the CB of ZIS is about -0.73 V, and the VB of Te is about 0.63 V (vs. NHE). In addition, according to the formula:

$$E_{CB} = \mathrm{E_{VB}} - \mathrm{E_g}$$

The VB of ZIS and the CB of Te can be confirmed as 1.54 and -1.36 V (vs. NHE), respectively.[4]

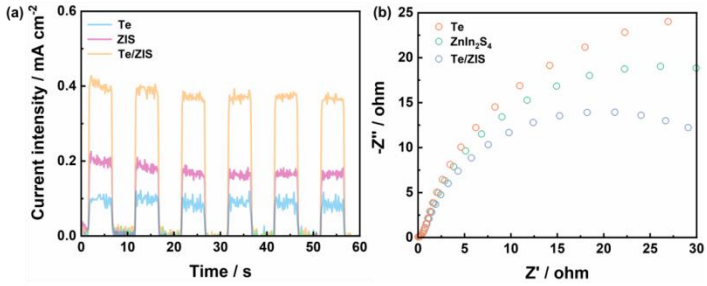

Fig. S12 (a) Photocurrent curves and (b) EIS spectra of Te/ZIS NLs, Te NWs and ZIS NPs under visible-light illumination.

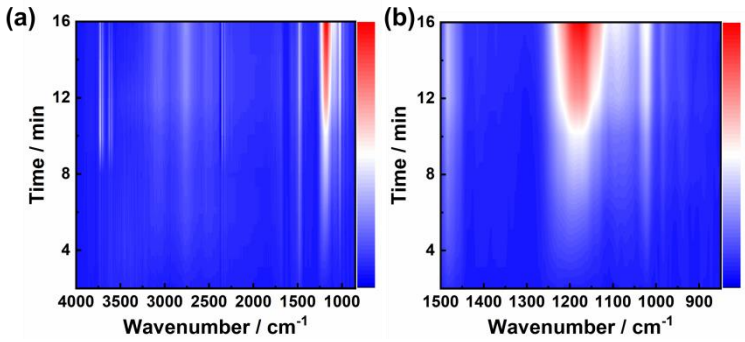

Fig. S13 Contour plots of in situ DRIFTS spectra for Te/ZIS NLs.

Table S1 Comparison of different catalysts for photocatalytic H_2O_2.

Samples	Light source	Reaction system	H_2O_2 yields (μmol g^{-1} h^{-1})
SnS_2/In_2S_3/CDs	λ ≥ 420 nm	H_2O	1112[1]
TDB-COF	λ ≥ 420 nm	H_2O	723.5[2]
PEI/C_3N_4	AM 1.5G	H_2O	208.1[3]
ZIS/PDA0.1	λ＞420 nm	H_2O	1747[4]
RF/P3HT-1.0	λ＞300 nm	H_2O	666[5]
K-CN/$ZnIn_2S_4$	λ＞420 nm	H_2O	1729.9[6]
DNM88B@ZIS	λ＞420 nm	H_2O	624.06[7]
PI/$ZnIn_2S_4$-2	λ＞420 nm	H_2O	411.07[8]
CdS/$ZnIn_2S_4$	λ＞400 nm	H_2O	604.8[9]
This work	**λ ≥ 420 nm**	**H_2O**	**1920**

References

1 G.-H. Moon and W. Choi, *Energy Environ. Sci.*, 2014, 7, 4023.

2 Z. Zhou and Y. Shen, *Appl. Catal. B*, 2023, 334, 122862.

3 X. K. Zhang and L. Yue, *ACS Catal.*, 2020, 10, 3697-3706.

4 S. Huang and J. Y. Gao, *ACS Appl. Nano Mater.*, 2024, 7, 4481-4490.

5 Y. Shiraishi and T. Hirai, *J. Am. Chem. Soc.*, 2021, 143, 12590.

6 S. Q. Zeng and L. N. Li,*ACS Sustainable Chem. Eng.*, 2023, 11, 7094.

7 M. Liu, and W. Zhou, *J. Hazard. Mater.*, 2022, 437, 129436.

8 X. Liu and X. Zhang, *Appl. Surf. Sci.*, 2024, 643, 158637.

9 E. Zhang and K. Ariga, *Appl. Catal. B*, 2021, 293, 120213.